

Article

Not peer-reviewed version

Dendroanatomy and Seasonal Hydroclimatic Responses of Long-Lived Yellow Pines (*Pinus jeffreyi* and *P. ponderosa*) in the Tahoe Basin of the Sierra Nevada, USA

Alexis D. Rodriguez , [Emanuele Ziaco](#) , [David M. Meko](#) , [Franco Biondi](#) *

Posted Date: 8 May 2026

doi: 10.20944/preprints202605.0486.v1

Keywords: quantitative wood anatomy; dendroclimatology; xylem traits; tracheid measurements; montane conifers; tree rings



Preprints.org is a free multidisciplinary platform providing preprint service that is dedicated to making early versions of research outputs permanently available and citable. Preprints posted at Preprints.org appear in Web of Science, Crossref, Google Scholar, Scilit, Europe PMC, OpenAlex.

Copyright: This open access article is published under a [Creative Commons CC BY 4.0 license](#), which permit the free download, distribution, and reuse, provided that the author and preprint are cited in any reuse.

Disclaimer/Publisher's Note: The statements, opinions, and data contained in all publications are solely those of the individual author(s) and contributor(s) and not of MDPI and/or the editor(s). MDPI and/or the editor(s) disclaim responsibility for any injury to people or property resulting from any ideas, methods, instructions, or products referred to in the content.

Article

Dendroanatomy and Seasonal Hydroclimatic Responses of Long-Lived Yellow Pines (*Pinus jeffreyi* and *P. ponderosa*) in the Tahoe Basin of the Sierra Nevada, USA

Alexis D. Rodriguez ¹, Emanuele Ziaco ², David M. Meko ³ and Franco Biondi ^{1,*}

¹ DendroLab, Department of Natural Resources and Environmental Science, University of Nevada, Reno, NV 89557, USA

² Department of Geography, Johannes Gutenberg Universität, 55122 Mainz, Germany

³ Laboratory of Tree-Ring Research, The University of Arizona, Tucson, AZ 85721, USA

* Correspondence: franco.biondi@dendrolab.org; Tel.: +1 (775) 784-6921

Abstract

Because wood anatomical traits and tree-ring features vary with species and climatic regime, cellular-scale measurements complement ring-width chronologies and help with understanding how forests may respond to future environmental change. We developed anatomical chronologies spanning the 1900-2019 period from multi-century old yellow pines (*Pinus jeffreyi* Balf. and *P. ponderosa* P & C Laws.) at four sites surrounding the Tahoe Basin of the Sierra Nevada, at the border between Nevada and California, USA. Measurements of earlywood and latewood traits included lumen area, lumen length, lumen width, wall length, wall-to-lumen length ratio, and conductive area. Climate sensitivity was estimated by bootstrapped response functions with precipitation and temperature (monthly and seasonal) from the Global Historical Climate Network interpolated to the site locations. Moisture emerged as the primary control on anatomical trait expression, as significant coefficients involved precipitation rather than temperature. Earlywood lumen size and conductive capacity were associated with late-winter through spring moisture, while cellular wall characteristics were connected with conditions during the growing season. Overall, our study provided new insights into the potential impacts of climatic changes on woody species of remarkable size and longevity in an area that is prized for its natural beauty and scenic mountain landscapes.

Keywords: quantitative wood anatomy; dendroclimatology; xylem traits; tracheid measurements; montane conifers; tree rings

1. Introduction

Dendrochronology is a tool that allows for the reconstruction of past climate events recorded by tree growth and provides insights into quantifying drought impacts [1], assessing fire regimes [2], and analyzing tree responses to environmental stressors across space and time [3]. While ring widths have been regarded as the basic unit of annual radial growth in trees, they can be partitioned into earlywood and latewood, a seasonal division that allows for better insight into the physiological processes responsible for tree growth and its environmental drivers [4,5]. Xylogenesis, i.e. wood formation, results in characteristic anatomical differences during the growing season, such as, for conifers of temperate climates, earlywood tracheids with larger lumens and thinner cell walls than latewood tracheids [6]. Ultimately, combining cellular-scale features with classic tree-ring proxies is expected to improve dendroclimatic reconstructions, and can help with predicting forest responses to future environmental change [7].

In the northern Sierra Nevada, between California and Nevada, the upper reaches of the Truckee River watershed are occupied by the Lake Tahoe Basin, which spans high elevations of approximately 1900-3350 m and exhibits a Mediterranean montane climate, with cold, wet winters and warm, dry summers [8]. Vegetation is characterized by mixed coniferous forests with varying stand composition and structure [9]. Prior to Euro-American settlement, these forests were shaped by frequent low- to moderate-intensity fires, resulting in open-grown stands dominated by old, large-diameter trees [10]. Widespread logging during the Comstock mining era (1870-1900), followed by sustained long-term fire suppression throughout the 20th century, and often continuing until the present, have produced dense stands with altered species composition and structure [11]. For the drought-tolerant, fire-adapted yellow pines (*Pinus ponderosa* P. & C. Laws. and *Pinus jeffreyi* Balf.), the post-Comstock changes likely increased competition and canopy closure, reducing light availability and intensifying moisture stress, with potential consequences for xylem traits such as lumen size and cell-wall thickness [12].

Conifer wood formation reflects a pronounced seasonal trade-off in xylem structure, with tracheid lumen dimensions and wall investment shifting across each ring to balance hydraulic efficiency and safety [6,13]. Seasonal variation in lumen area and wall thickness tracks climate conditions and underscores the importance of embolism risk under seasonal water stresses such as drought and freeze-thaw events [14,15]. In Argentinian ponderosa pine, drought typically reduces growth more than hydraulic function, producing smaller lumens and thinner walls without significantly altering whole-ring conductivity [16]. Similar responses in other conifers led to reduced lumen area and higher wall-to-lumen length ratios in dry years [17]. Structural traits such as lumen size and wall length/thickness interact with hydraulic architecture to modulate xylem resistance, with taller trees and those under prolonged drought relying on these adjustments to maintain water transport while balancing safety [18–20].

Studies on Great Basin conifers have showed that wood anatomical development in snow-dominated mountain climates usually results in greater cell lumens and conductive area as winter precipitation increases, while summer drought reduces lumen sizes and leads to thicker cell walls [21,22]. Xylogenesis of ponderosa pine, however, can be extremely variable under drought-prone conditions [23]. Although vulnerability of ponderosa pine to xylem cavitation remained similar under various climatic conditions, in warmer and drier environments this species exhibited a higher specific hydraulic conductivity, associated with larger lumen diameters [24]. Additional research has evaluated how hydraulic characteristics of ponderosa pine vary with tree age, growth rate, and internal stem structure, including axial and radial patterns in conductivity, water storage, and native embolism [18,25].

As the conservation of natural resources has become a top priority for land managers, the ecological values of long-lived trees has gained world-wide interest, especially in mountain ecosystems [3,26]. Mature forests and their extremely old trees are not rare in the topographically complex western USA, although the physiological processes, life history strategies, and environmental adaptations of ancient trees are not necessarily the same as those that are investigated in a greenhouse or in other highly controlled settings, as it has been observed, for instance, in terms of growth rates and carbon accumulation potential [27]. Trees of impressive size and/or age are examples of charismatic megafauna [28] that remain visible in the landscape throughout multiple human generations, thereby becoming intimately linked with socio-economic structures, traditional customs and spiritual beliefs (e.g., [29]). Their presence can also become a synonym of sustainable land stewardship, which is currently being challenged in many areas of the western USA, including the Lake Tahoe Basin, by increasing suburban and exurban development [30].

In this study, we used quantitative wood anatomy to examine how seasonal climate variability shapes xylem development in dominant and codominant, multi-century old yellow pines around the Tahoe Basin, an area that is prized for its natural beauty and scenic mountain landscapes. Specifically, we evaluated how six anatomical traits, namely lumen area (LA), lumen length (LL), lumen width (LW), average cell-wall thickness (WL), wall-to-lumen length ratio (WLLL), and conductive area

(CA), respond to seasonal patterns of temperature and precipitation, with particular emphasis on possible differences between earlywood and latewood traits. Our main objective was to improve our understanding of growth patterns in trees of remarkable size and longevity, and to clarify how intra-annual wood formation is anatomically adjusted to seasonal climate variation.

2. Materials and Methods

2.1. Dendrochronological Field Sampling and Laboratory Processing

Wood increment cores were collected from August to November, 2020, at four forest sites in the upper reaches of the Truckee River watershed, around the Tahoe Basin (Figure 1; Table 1). Two sites are at higher elevations (~2400-2500 m) and two at lower elevations (~2000 m); one high-elevation site and one low-elevation site are in California, on the west slope of the Sierra Nevada, and the other two sites are in Nevada, closer to the boundary with the Great Basin and therefore relatively warmer and drier because of the rain shadow effect [31]. A total of 53 mature yellow pines were sampled and their increment cores were used to develop crossdated site chronologies [32]. Two wood cores, each ~5 mm in diameter, were collected from every tree, at ~1.3 m from the ground, on opposite sides of the stem, and along the slope contours, using a standard increment borer to ensure minimal wounding and consistent radial sampling from the bark inward. Dominant trees with minimal defects either in the crown or on the trunk were selected, with a preference for individuals with signs of old age, including large branches and spiked tops (Figure S1).

Table 1. Study site information, including species code (PIJE = *Pinus jeffreyi*, PIPO = *Pinus ponderosa*) and geographical coordinates.

Site Name	Site Code	State	Species	Lat. (°N)	Long. (°W)	Elev. (m)
Little Valley	LTV	Nevada	PIJE	39.24781	119.87456	2006
Lemon Canyon Road	LEM	California	PIJE	39.56024	120.24669	2008
Luther Pass	LUR	California	PIJE	38.79548	119.98629	2397
Chimney Peak / Mt. Rose	CPR	Nevada	PIPO	39.45645	119.95361	2507

In the laboratory, increment cores were mounted on grooved wooden supports, and progressively sanded with fine-grit sandpaper to enhance visibility of growth ring boundaries. All samples were crossdated visually under a zoom-stereoscope binocular microscope at 10-30x magnification. Core surfaces were digitized at 2400 dpi optical resolution using an Epson Expression 12000XL-GA professional scanner. Early- and late-wood widths were then measured on the scanned images using the CooRecorder/CDendro software (v.9.6; <http://www.cybis.se/forfun/dendro/>), followed by statistical quality control using the COFECHA software [33]. Because anatomical sample processing and measurements are extremely time-intensive, at each site we selected five increment cores (Table 2) that showed high correlations with the overall site chronology (Table S2) for further cellular-level analyses.

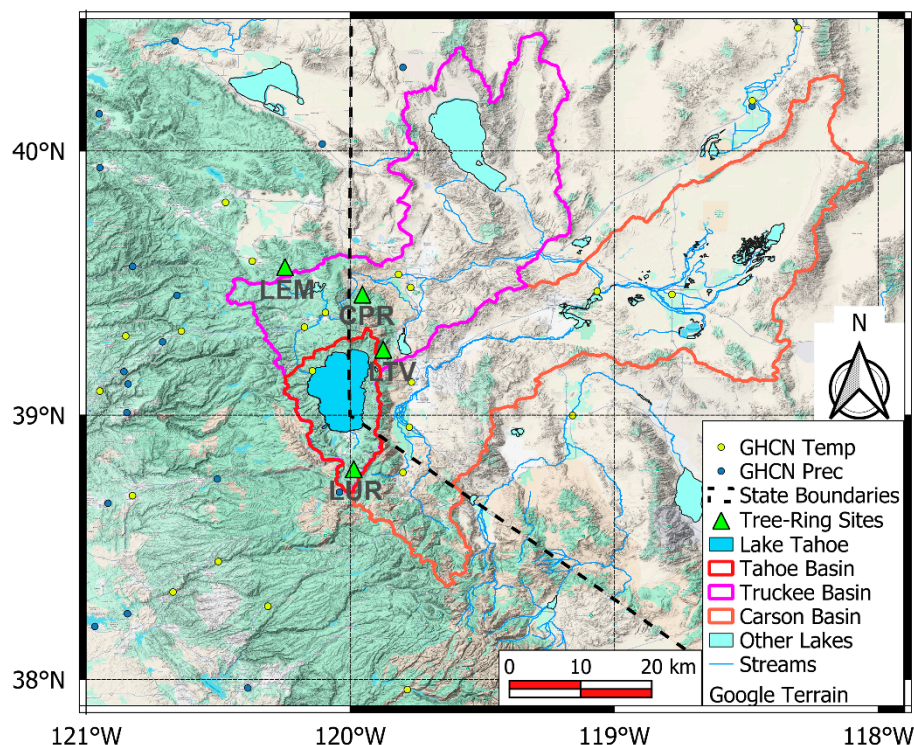


Figure 1. Map of the study area and tree-ring sampling sites (green upper triangles; Table 1) in the upper reaches of the Truckee River Basin (magenta boundary), next to the Carson River Basin (orange boundary) and surrounding the Lake Tahoe Basin (red boundary). State borders (black dashed lines) and stations included in the Global Historical Climate Network (GHCN) that were used to obtain site-specific air temperature (yellow dots) and precipitation (blue dots) are also shown.

Table 2. Summary information for the wood increment cores that were selected for cellular-level measurements at each site (see Table 1)*.

Site Code	Tree DBH (cm)	Tree Age (yr)	Mean Width (mm)	Stand. Dev. (mm)	Site Corr.
LTV	63-83	391-603	0.39-0.61	0.13-0.33	0.58-0.70
LEM	76-92	190-480	0.83-1.64	0.73-0.81	0.73-0.81
LUR	109-160	267-499	0.64-1.35	0.22-0.72	0.54-0.67
CPR	101-164	288-548	0.74-1.41	0.36-0.46	0.70-0.75

* All reported values are ranges (min-max). Five cores were selected at each site, but only three of them were measured for CPR. DBH: diameter at breast height (~1.3 m from the ground). Age: number of rings in the wood increment core. Mean Width: average ring width. Stand. Dev.: standard deviation of the ring widths. Site Corr.: linear correlation with the master chronology produced by the COFECHA software.

2.2. Anatomical Measurements

Rings going back to the year 1900 were removed from the core mounts, cleaned of resin and other chemicals using automated baths in progressively increasing concentrations of ethanol and PROTOCOL SafeClear, and finally embedded in paraffin to stabilize the tissues prior to microsectioning. Sections approximately 15- μ m thick were then cut using an automated sliding microtome. These sections were stained with Safranin, which differentially colors lignified and non-lignified tissues. Stained slides were mounted using Canada balsam, dehydrated, and finally digitized using a high-resolution microscope-camera system under consistent 10x magnification [34].

Wood anatomical traits were measured using the WinCELL™ Pro software (v. 2020a, 64-bit; <https://www.regentinstruments.com>) and then compiled using the XLCell macro for the Microsoft

Office Excel spreadsheet. The six key anatomical traits (Figure S2) were lumen area (LA, μm^2); lumen length (LL, μm), measured along the tracheid path; lumen width (LW, μm), measured perpendicular to LL and across the lumen centroid; wall length (WL, μm), representing the mean wall thickness measured on the two sides of the lumen along the tracheid path; wall-to-lumen length ratio (WLLL, unitless), calculated as WL/LL ; and conductive area (CA, μm^4), where $CA = \left(\frac{LL+LW}{2}\right)^4$ [35]. Because tracheid lumens are often irregular, as opposed to perfectly circular, LL and LW were retained as separate variables rather than being treated as a single diameter. Moreover, their average elevated to the fourth power, i.e. CA, is such that larger conduits contribute disproportionately more to potential transport capacity than smaller conduits, and can be interpreted as a rough approximation of the Hagen-Poiseuille formula for flow rate through an irregularly shaped conduit [36]. In other words, CA captures variation in the size-related conductive potential of tracheids without constituting a direct measurement of water flow. Measurements were taken along five-six radial paths per growth ring, calibrated from the imagery scale, and averaged by year. Earlywood and latewood were separated according to the Mork criterion [37], whereby a tracheid was classified as latewood when $2 \times WL \geq LL$; tracheids not meeting this threshold were classified as earlywood.

2.3. Dendroclimatic Analysis

Climate data were obtained from the Global Historical Climatology Network (GHCN), provided by the National Oceanic and Atmospheric Administration's (NOAA) National Centers for Environmental Information (NCEI). The GHCN dataset includes land-based stations spanning the period from 1832 to the present, with records from over 100,000 stations across 180 countries and territories [38]. Monthly average air temperature and total precipitation (GHCNm) were downloaded from 32 temperature and 73 weather stations closest to our study sites, and then interpolated to our site locations using inverse distance weighting in order to accurately represent climatic conditions relevant to our analysis [39]. Seasonal predictors were defined as mean temperature and summed precipitation for the cool-wet season (from the previous-year October to the current-year May) and the warm-dry season (from June to September of the current year).

Median chronologies were calculated by year for the six anatomical variables (LA, LL, LW, WL, WLLL, CA), separately for earlywood and latewood and by pooling all available measurements from the four study sites. Cellular chronologies were not detrended because climatic relationships may otherwise be less clearly identifiable [40]. Monotonic temporal trends were evaluated by means of the non-parametric Mann-Kendall test [41,42] applied to the standardized median chronologies. The four sampling sites were characterized by similar climatic regime, albeit with different average values (Figure S3 and Table S1), which were related to their elevation and proximity to the rain-shadow of the eastern Sierra Nevada. Since cellular-level measurements from the four sites were pooled together, site climate records were also combined by taking the median value of monthly precipitation and air temperature timeseries.

Dendroclimatic analyses started in 1940, given the relatively low number of climate records available during the first few decades, and ended in 2019, the last complete year of wood anatomical measurements. Connections with air temperature and precipitation, either monthly, seasonal or in multi-month combinations, were investigated using bootstrapped response functions and partial correlations, both available in the R package *treeclim* [43]. Partial correlation analysis was applied to test the seasonal associations of each anatomical chronology with climate using adjacent one-, three-, and six-month long windows. Partial correlation coefficients were calculated using both precipitation and temperature and alternatively choosing one or the other as primary variable [44]. All calculations were performed using a combination of the R numerical environment [45], MATLAB [46], and SAS [47].

3. Results

3.1. Anatomical Chronologies

Significant differences were found between earlywood (EW) and latewood (LW) cellular properties from 1900 to 2019 (Table 3 and Figure S4). Earlywood lumen dimensions were consistently greater than latewood ones, reflecting the functional distinction in conduit size during the growing season. Latewood LA remained about 81% lower than earlywood LA and exhibited lower interannual variability over time. Earlywood lumen length (LL) was overall about 3.7 times greater than latewood LL, which also had lower interannual variability and fluctuated across a narrower absolute range. Notably, latewood lumen width (LW) was narrower but showed greater interannual variability than earlywood LW. Median cell wall length (WL) was about 28% greater in latewood than in earlywood, which had lower interannual variability, although WL remained within relatively narrow ranges in both EW and LW. The wall-to-lumen length ratio (WLLL) was consistently greater in latewood than in earlywood, indicating proportionally thicker walls relative to lumen size later in the growing season. Latewood WLLL was about 6.5 times greater than earlywood WLLL and fluctuated across a wider absolute range. Conductive area (CA) was consistently much greater in earlywood than in latewood, reflecting the dominant role of early-season conduits for water transport. Latewood CA was about 93% smaller and with lower interannual variability than earlywood CA.

Table 3. Summary statistics* for the six xylem anatomical variables measured from 1900 to 2019 (see Figure S4) at the four study sites (CPR, LEM, LTV and LUR; see Table 1): Lumen Area (LA, μm^2), Lumen Length (LL, μm), Lumen Width (LW, μm), Wall Length (WL, μm), Wall-to-Lumen Length ratio (WLLL, unitless), and Conductive Area (CA, μm^4). Earlywood (EW) vs. latewood (LW) average values were always significantly different ($p < 0.001$) using two-sided t-tests.

Variable	CPR		LEM		LTV		LUR		Median	
	EW	LW	EW	LW	EW	LW	EW	LW	EW	LW
LA	833 ± 137	163 ± 31	975 ± 130	166 ± 18	906 ± 80	175 ± 14	972 ± 61	197 ± 18	932 ± 57	177 ± 8
LL	31 ± 3	9 ± 1	32 ± 3	8 ± 0.5	30 ± 2	8 ± 0.5	33 ± 1	9 ± 0.7	31 ± 2	8 ± 0.4
LW	29 ± 2	20 ± 2	34 ± 2	21 ± 2	32 ± 1	22 ± 2	32 ± 1	23 ± 1	32 ± 0.7	22 ± 1.0
WL	3 ± 0.4	4 ± 0.6	3 ± 0.3	5 ± 0.6	3 ± 0.2	4 ± 0.5	3 ± 0.2	4 ± 0.4	3 ± 0.1	4 ± 0.3
WLLL	0.1 ± 0.01	0.7 ± 0.19	0.1 ± 0.02	0.9 ± 0.16	0.1 ± 0.01	0.7 ± 0.11	0.1 ± 0.01	0.7 ± 0.09	0.1 ± 0.01	0.8 ± 0.07
CA	1135534 ± 498521	67038 ± 26528	1443537 ± 357370	89180 ± 20309	1161894 ± 191154	90087 ± 15796	1390710 ± 179412	106209 ± 17680	1300119 ± 159703	90517 ± 9521

* Mean ± Standard Deviation.

Linear correlations between standardized median chronologies from 1940 to 2019 (Figures 2 and 3) revealed asynchronous patterns between earlywood and latewood for most anatomical trait (r from -0.14 to 0.07) except wall length ($r = 0.51$) and lumen length ($r = 0.34$). Conduit dimensions (LA, LW, LL, CA) were more correlated in the earlywood (r from 0.31 to 0.98) than in the latewood (r from non-significant to 0.68), although this could also be due to the much smaller, hence more difficult to measure, latewood sizes (Table 3). Wall-related dimensions (WL, WLLL) were instead more correlated in the latewood ($r = 0.67$) than in the earlywood ($r = 0.46$). Significant monotonic trends were present in most standardized anatomical chronologies (Table 4), although they were weaker during 1940-2019 than in the period 1900-2019 (except for latewood WLLL), and they were relatively minor compared to the amount of year-to-year variability (Figure 3).

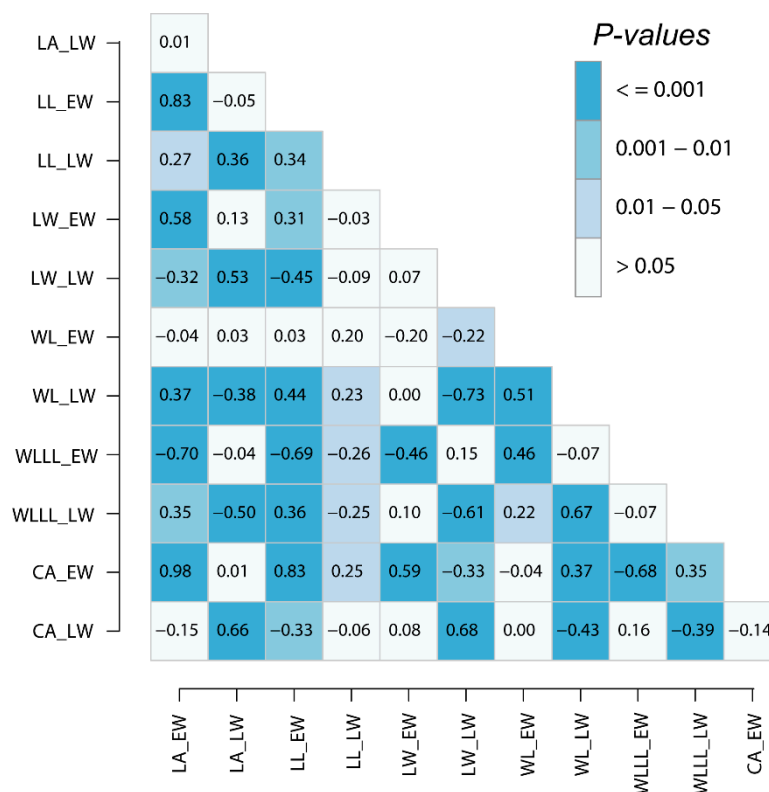


Figure 2. Linear correlations between the anatomical median chronologies (see Table 3 for the meaning of all abbreviations), expressed as Z-scores from 1940 to 2019.

Table 4. Summary of Mann-Kendall tests for monotonic trends[#] in standardized median anatomical chronologies (see Table 3 for the meaning of all abbreviations).

Variable	1900-2019		1940-2019	
	EW	LW	EW	LW
LA	-0.38***	0.05	-0.29***	-0.003
LL	-0.48***	-0.20***	-0.31***	-0.07
LW	-0.09	0.32***	-0.14	0.26***
WL	0.23***	-0.37***	0.11	-0.21**
WLLL	0.43***	-0.10	0.27***	-0.20**
CA	-0.37***	0.24***	-0.29***	0.08

[#]Significance: * $p < 0.05$; ** $p < 0.01$; *** $p < 0.001$.

3.2. Dendroclimatic Relationships

Response functions between anatomical variables and seasonal climate showed significant connections with precipitation, whereas none were found for temperature (Figure 4). For both earlywood and latewood, Oct-May precipitation was positively correlated with lumen length. Earlywood wall length was negatively related to Jun-Sep precipitation, which also had a negative influence on latewood wall-to-lumen length (Figure 4).

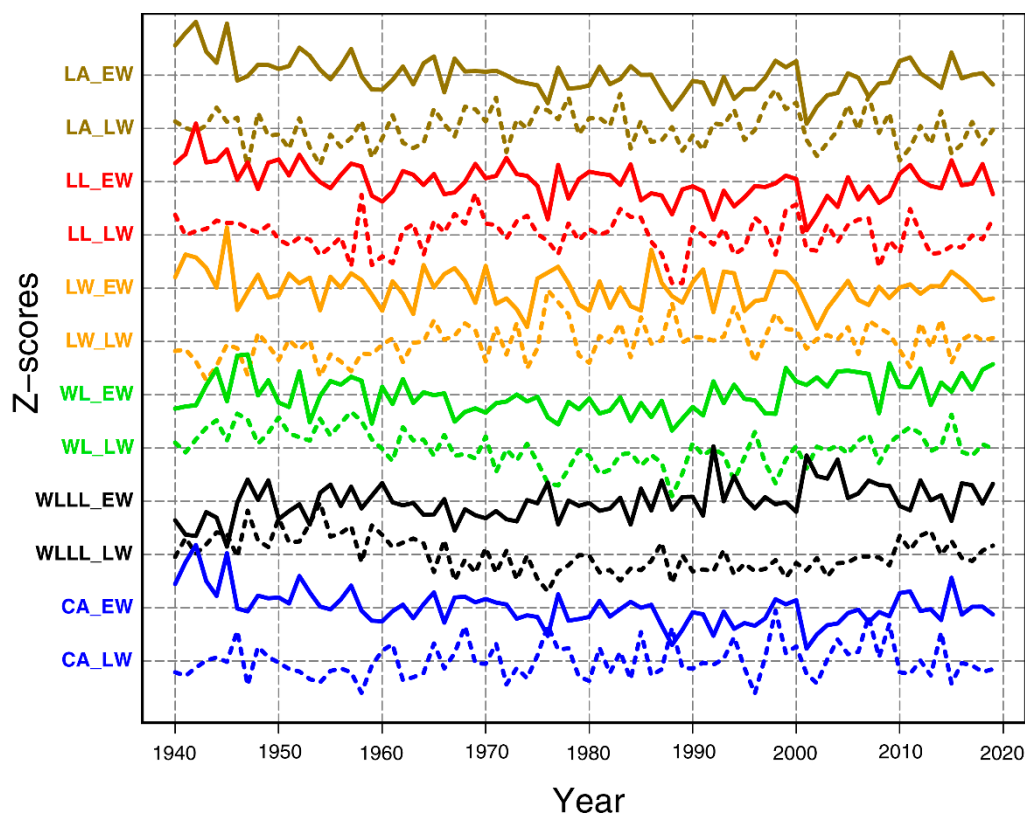


Figure 3. Timeseries plots of the six anatomical variables (Z-scores: standardized median chronologies; see Table 3 for the meaning of all abbreviations) used for investigating relationships with climate variables from 1940 to 2019.

Partial correlation analyses revealed a positive seasonal association between precipitation and earlywood lumen area across late winter and spring into early summer (Figure S4a). The strongest relationship was found for a, three-month period ending in July. Air temperature, on the other hand, showed the opposite pattern, with a negative influence in late spring, as shown by the significant single- and three-month-window May coefficient. For latewood LA, only January precipitation showed a positive correlation.

The positive connection between precipitation and lumen length (LL) was confirmed by analyses over 3- and 6-month windows; no connection with air temperature appeared (Figure S4a). For latewood LL, positive precipitation signals were found during the cool season, with the highest significant coefficients during the six-month intervals ending in February, March, and April. In contrast, temperature showed negative correlations with latewood LL, including single-month correlations in July, June, and March, three-month windows ending in April and October, and broader six-month spans ending in December, November, October, September, August, and July.

Earlywood lumen width (LW) was significantly correlated only with air temperature, with negative coefficients in May, in three-month windows ending in May and June, and in the six-month window ending in September (Figure S4a). Latewood LW, by contrast, was positively linked with both August precipitation and August air temperature. Negative correlations were observed with longer precipitation windows, i.e. six-month intervals ending in March, April, and May, as well as for the single-month December air temperature.

For earlywood wall length (WL), precipitation had a negative influence in June, in the three-month windows ending in August and July, and in the six-month interval ending in September. In contrast, May temperature showed a positive correlation with earlywood WL (Figure S4b). Latewood WL displayed no connection with temperature and only two precipitation relationships, one negative in September and one positive, but most likely spurious, with the six-month precipitation window ending in August of the previous year. Earlywood wall/lumen length (WLLL) showed a mixture of

precipitation and temperature relationships, the former negative and the latter positive (Figure S4b). For latewood WLLL, both precipitation and temperature in August had a negative influence, with additional negative precipitation relationships in the three-month windows ending in August and September.

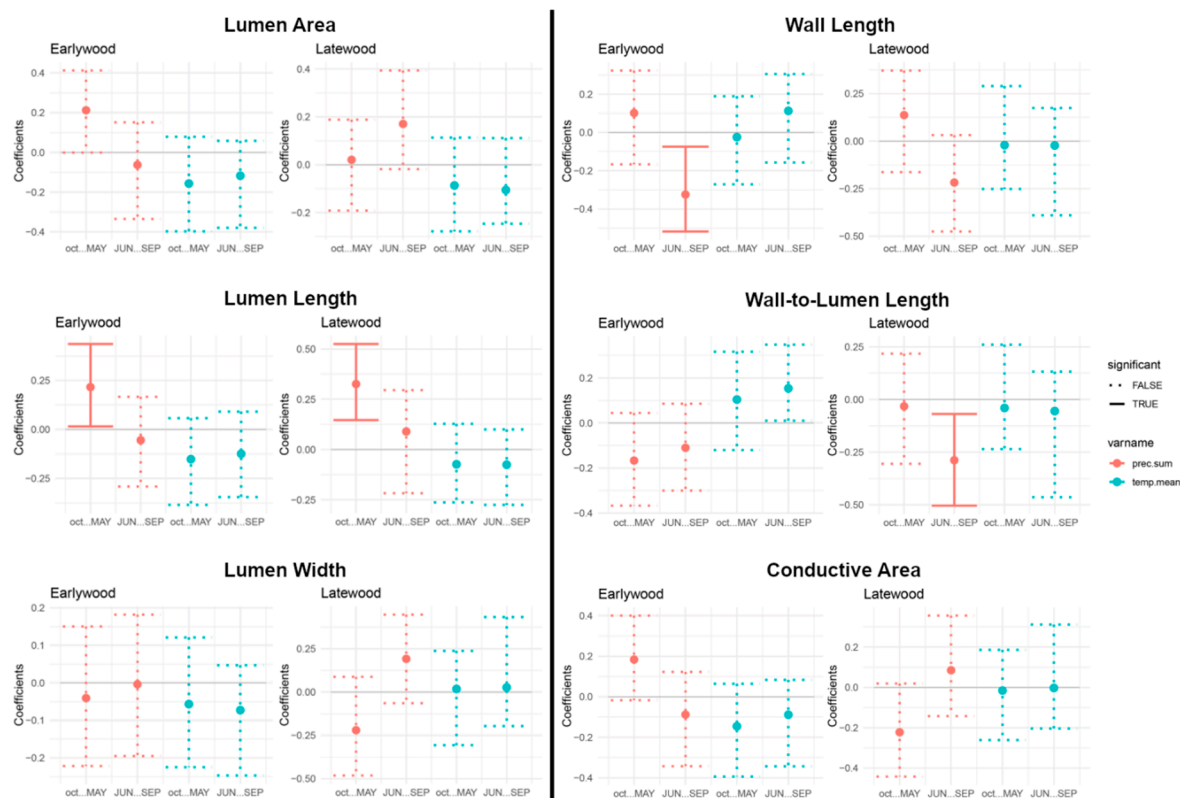


Figure 4. Response functions between 12 anatomical variables and seasonal climate from 1940 to 2019 obtained using the R package *treeclim*. Significant coefficients are shown with solid lines instead of dotted ones.

For earlywood conductive area (CA), the highest significant positive association with precipitation was found for the three-month window ending in July (Figure S4b). May temperature, however, showed a negative connection with earlywood CA. Latewood CA was negatively linked with April precipitation as well as with the three-month interval ending in June and the six-month intervals ending in May and April.

4. Discussion

Consistent with established hydraulic trade-offs, the anatomical patterns observed in mature yellow pines at our study sites showed that seasonal moisture availability strongly shaped xylem construction within the annual ring. In particular, the contrasting sensitivities of earlywood versus latewood traits indicated that conductive allocation (CA) and relative wall investment (WL and WLL) were temporally partitioned across the growing season. These findings expand upon prior work by suggesting that in snow-dominated montane systems, both cumulative moisture storage and the seasonal timing of precipitation set the conditions for cellular-level anatomical variation. This interpretation is also supported by the spatial arrangement of the study sites around the Lake Tahoe Basin, as two sites were located on the western slope of the Sierra Nevada, whereas two others were located closer to the Great Basin boundary, where conditions are relatively warmer and drier because of the rain shadow effect. This contrast in site location captured a hydroclimatic gradient across the basin, supporting the inference that moisture availability was an important control on xylem anatomical patterns. Similar moisture-driven anatomical responses have been reported in other

conifers, where seasonal water availability helps shape conduit dimensions, wall-related traits, and the timing of xylem development [7,23,48].

Anatomical time series highlighted clear differentiation between earlywood and latewood. This contrast is consistent with the general seasonal organization of conifer xylem, in which earlywood favors conductive space and latewood reflects greater wall investment and support [6]. Earlywood traits associated with lumen size and conductive capacity, including LA, LL, LW, and CA, were consistently greater than their latewood counterparts, whereas latewood was characterized by greater WL and WLLL, reflecting proportionally thicker walls relative to lumen size. Over the 1900-2019 period, anatomical traits showed significant long-term monotonic trends, although with different interannual variability. Earlywood lumen-related traits, particularly LA, LL, and CA, tended to decline through time, while earlywood WLLL increased, suggesting reduced earlywood conductive space and greater relative wall investment. In contrast, latewood trends were more mixed, with latewood LW increasing but latewood WL and recent WLLL declining.

While the reduction over time in earlywood lumen area may point to a gradual reduction in snow accumulation and available soil moisture at the beginning of the growing season [49], time-series patterns among sites were not highly synchronous, either because of the relatively small sample size at each site or because interannual variation was influenced by local site conditions and microsite differences. Furthermore, even traits with significant trends fluctuated above and below their long-term means, indicating that year-to-year variability remained an important component of the anatomical record. Pairwise correlations between anatomical variables showed that lumen-based traits generally varied together in the earlywood, while wall-related features were more related in the latewood. This pattern is consistent with a functional trade-off between conductive capacity and relative wall investment, suggesting that wood anatomical structure remained broadly stable over the 20th century while year-to-year fluctuations reflected seasonal climatic variability superimposed on trait-specific and site-specific controls.

Multi-month dendroclimatic analyses clarified how xylem development is seasonally structured, with cell lumen and wall investments responding at different times of the year. Greater cool-wet season precipitation prior to and near the onset of spring cambial activity was associated with greater lumen length (LL), indicating that cell expansion in both earlywood and latewood was supported by soil-water reserves recharged early in the water year and made accessible in spring, when improved tree water status helps sustain cambial activity and tracheid enlargement, as opposed to relying solely on immediate spring precipitation. Comparable links between antecedent moisture, cambial activity, and subsequent cell enlargement have repeatedly been reported in drought-prone conifers [23,48,50].

Cellular wall traits were clearly connected with the warm-dry season. Wetter summers were associated with reduced wall thickness relative to lumen size in earlywood and lower latewood WLLL ratios, consistent with conditions that favor conductive efficiency, whereas drier summers likely promote greater allocation to WL relative to lumen size, enhancing hydraulic safety. The lack of significant temperature responses suggests that temperature influenced xylem formation indirectly, possibly through effects on snowpack accumulation, melt timing, and evaporative demand, while precipitation showed more direct correlations with anatomical traits. These results emphasize moisture availability as a primary seasonal control on how xylem structure is built and partitioned within the annual ring in this montane setting.

Latewood LL showed the clearest evidence for cool-season moisture control, with multiple significant precipitation windows spanning from winter through spring and into early summer. This response suggested that latewood tracheid growth was supported by moisture accumulated over preceding months, consistent with dependence on stored soil water that persisted beyond individual storms and continued to supply developing cells later in the season. In contrast, latewood LA displayed a comparatively narrow precipitation response, indicating that lumen area in latewood was less broadly responsive than latewood LL, and that different components of latewood anatomy can be regulated by distinctly time-dependent constraints.

Air temperature relationships with earlywood were comparatively limited, but directionally important. The significant negative May temperature relationships for earlywood LA and CA suggests that warmer spring conditions can constrain hydraulic investment, likely by increasing atmospheric demand and transpiration, reducing tissue water potential, or shifting phenology so that cell growth occurs under less favorable moisture conditions. Warmer spring conditions may not directly constrain growth through thermal limitation but can indirectly restrict xylem expansion by reducing plant water status during the earlywood enlargement phase [51].

The WL and WLLL ratios highlighted structural trade-offs within the xylem. Earlywood WL exhibited significant negative precipitation effects primarily during summer windows, indicating reduced wall thickness relative to lumen size under wetter conditions when hydraulic safety demands are relaxed. Similar drought-related shifts toward reduced lumen development and greater relative wall investment have been reported in other conifers, including high-elevation Great Basin species and ponderosa pine under water limitation [16,21]. Such shifts are consistent with broader interpretations of xylem adjustment under hydraulic stress, in which reduced conductive space and greater relative wall investment contribute to a safer but less efficient structure [19,20].

The earlywood WLLL ratio showed a consistent pattern of negative precipitation and positive temperature effects, implying that wet conditions favor proportionally greater conductive space, whereas warmer conditions are associated with greater wall thickness relative to lumen size. This response may also reflect shifts in cell expansion, wall deposition, or timing of xylem maturation under warmer and drier conditions. Latewood WLLL ratio and latewood LW both showed sensitivity to late-summer climate, especially August conditions, indicating that constraints during the latewood formation period can shape how trees balance conductivity and support. Negative August influences on the latewood WLLL ratio for both precipitation and temperature suggest that late-season conditions may drive the relative allocation to wall material versus lumen space during a critical phase of xylem maturation. Meanwhile, the mixed signals in latewood LW, with positive August precipitation and temperature but negative longer precipitation windows, further emphasize that the timing of moisture inputs matters, and that short-term conditions during latewood formation can have different implications than cumulative preceding moisture. This pattern is consistent with the view that latewood maturation is sensitive to short-term late-season conditions, when shifts in water status can alter the balance between lumen expansion and wall deposition [51,52].

Earlywood conductive area (CA) increased with multi-month precipitation windows, consistent with earlywood's primary role in maximizing hydraulic capacity when water is available, while the negative May temperature relationship supports the idea that warming-driven evaporative demand can suppress hydraulic investment. In latewood, CA showed negative precipitation responses over select windows, consistent with latewood contributing less to conductivity than earlywood and with anatomical adjustment during latewood formation being shaped by different functional priorities. In ponderosa pine, larger lumens have been associated with higher hydraulic conductivity even where vulnerability to cavitation did not differ across climates [24], but more recent work in the Great Basin pines suggests that hydraulic efficiency in pine species is more closely tied to growth than hydraulic safety under drought-prone conditions [36]. These results showed that anatomical adjustments in old-growth yellow pines were seasonally structured, with earlywood responding most strongly to late winter and spring moisture, and latewood traits responding to a combination of cool-season moisture integration and late-summer climatic conditions that shaped allocation during latewood formation.

5. Conclusions

Around the Lake Tahoe Basin, our quantitative wood anatomy results show that old-growth yellow pines express a seasonally structured hydraulic trade-off in xylem allocation strategies. Overall, moisture availability emerged as the primary control on anatomical trait expression, with precipitation-driven snow-pack and soil-water storage setting the conditions for cell expansion and subsequent wall investment. Earlywood lumen traits (LA, LL) and CA responded most consistently

to late-winter through spring moisture, indicating that early-season tracheid enlargement integrates both immediate inputs and accumulated water availability carried into the growing season, while latewood traits were more timing-dependent and reflected tighter constraints during late-season formation and maturation. Cellular wall metrics (WL, WLLL) further highlighted wetter conditions associated with greater hydraulic capacity and warmer conditions associated with relatively greater wall investment.

In the Sierra Nevada, snowpack typically acts as a natural reservoir, gradually releasing water into soils through late spring and early summer. During the period of instrumental records, earlier snowmelt has caused peak streamflow to advance by 1-4 weeks across the western U.S., including the Tahoe Basin, either because of warming temperatures [53], precipitation shifting from snow to rain [54], or increased dust depositions [55]. As land managers and policy managers grapple with the complex interactions that drive ecosystem dynamics in complex terrain, our study provided new insights into the potential impacts of climatic changes on woody species of remarkable size and longevity in an area that is prized for its natural beauty and scenic mountain landscapes.

Supplementary Materials: The following supporting information can be downloaded at the website of this paper posted on Preprints.org, Figure S1: The largest (DBH of 164 cm) and second oldest (548 years on the longest core) yellow pine that was sampled at the four study sites is this ponderosa pine from CPR; Figure S2: Representative transverse wood microsection showing anatomical measurements; Figure S3: Timeseries plots of the water-year (from previous October to current September, 1895 to 2021) total precipitation (Precip) and mean air temperature (Temp) interpolated at the four sampling sites (Table 1) from GHCN and PRISM data (see text for details); Figure S4: Timeseries plots of the six anatomical variables (see Table 3 for summary statistics and variable units) that were measured from 1900 to 2019 at the four study sites (CPR, LEM, LTV and LUR; see Table 1); Figure S5: Seasonal dendroclimatic analysis used to quantify relationships between anatomical and climate variables; Table S1: Summary of interpolated climate variables at the four study sites (Figure 1 and Table 1) for the 1940-2019 period; Table S2: Summary of tree-ring data obtained from all yellow pines that were cored at the study sites (see Table 1).

Author Contributions: Conceptualization, F.B. and A.D.R.; methodology, F.B., E.Z. and D.M.M.; software, A.D.R.; validation, F.B., E.Z. and D.M.M.; formal analysis, A.D.R. and F.B.; investigation, F.B.; resources, F.B.; data curation, F.B.; writing—original draft preparation, A.D.R.; writing—review and editing, F.B., E.Z. and D.M.M.; visualization, A.D.R. and F.B.; supervision, F.B. and E.Z.; project administration, F.B.; funding acquisition, F.B. and D.M.M.. All authors have read and agreed to the published version of the manuscript.

Funding: This research was funded by the US National Science Foundation (grant AGS-P2C2-1903561 to F.B. and AGS-P2C2-1903535 to D.M.M.). A.D.R. was funded by a Teaching Assistantship from the Department of Natural Resources and Environmental Science as well as from the Graduate Dean's Merit Scholarship at the University of Nevada, Reno. F.B. was funded in part by the Experiment Station of the College of Agriculture, Biotechnology, and Natural Resources at the University of Nevada, Reno.

Data Availability Statement: The original contributions presented in this study are included in the article/supplementary material. The raw data supporting the conclusions of this article will be made available by the corresponding author upon request.

Acknowledgments: F.B. is grateful for the help received during field work from Xinsheng Liu, Hugh Safford, and Maddy Fontaine. All laboratory measurements were performed by Emily Dietrick with training and supervision provided by E.Z. and F.B.. A.D.R. is grateful to Hall Cushman and Felipe Barrios-Masias for their support, guidance, and feedback.

Conflicts of Interest: The authors declare no conflicts of interest. The funders had no role in the design of the study; in the collection, analyses, or interpretation of data; in the writing of the manuscript; or in the decision to publish the results.

References

- Meko, D.M.; Woodhouse, C.A. Tree-ring footprint of joint hydrologic drought in Sacramento and Upper Colorado river basins, western USA. *J. Hydrol.* **2005**, *308*, 196-213, doi:10.1016/j.jhydrol.2004.11.003.
- Biondi, F.; Jamieson, L.P.; Strachan, S.; Sibold, J. Dendroecological testing of the pyroclimatic hypothesis in the central Great Basin, Nevada, USA. *Ecosphere* **2011**, *2*, art. 5 (20 pp.), doi:10.1890/es10-00068.1.
- Piovesan, G.; Biondi, F. On tree longevity. *New Phytol.* **2021**, *231*, 1318-1337, doi:10.1111/nph.17148.
- Friend, A.D.; Eckes-Shephard, A.H.; Fonti, P.; Rademacher, T.T.; Rathgeber, C.B.K.; Richardson, A.D.; Turton, R.H. On the need to consider wood formation processes in global vegetation models and a suggested approach. *Ann. For. Sci.* **2019**, *76*, 49, doi:10.1007/s13595-019-0819-x.
- Rossi, S.; Anfodillo, T.; Čufar, K.; Cuny, H.E.; Deslauriers, A.; Fonti, P.; Frank, D.C.; Gričar, J.; Gruber, A.; Huang, J.-G.; et al. Pattern of xylem phenology in conifers of cold ecosystems at the Northern Hemisphere. *Glob. Change Biol.* **2016**, doi:10.1111/gcb.13317.
- Larson, P.R. *The Vascular Cambium: Development and Structure*; Springer-Verlag: Berlin, Germany, 1994.
- Fonti, P.; von Arx, G.; García-González, I.; Eilmann, B.; Sass-Klaassen, U.G.W.; Gärtner, H.; Eckstein, D. Studying global change through investigation of the plastic responses of xylem anatomy in tree rings. *New Phytol.* **2010**, *185*, 42-53, doi:10.1111/j.1469-8137.2009.03030.x.
- Coats, R. Climate change in the Tahoe basin: regional trends, impacts and drivers. *Clim. Change* **2010**, *102*, 435-466, doi:10.1007/s10584-010-9828-3.
- Taylor, A.H. Identifying forest reference conditions on early cut-over lands, Lake Tahoe basin, USA. *Ecol. Appl.* **2004**, *14*, 1903-1920, doi:10.1890/02-5257.
- Beaty, R.M.; Taylor, A.H. Fire disturbance and forest structure in old-growth mixed conifer forests in the northern Sierra Nevada, California. *J. Veg. Sci.* **2007**, *18*, 879-890, doi:10.1111/j.1654-1103.2007.tb02604.x.
- Beaty, R.M.; Taylor, A.H. Fire history and the structure and dynamics of a mixed conifer forest landscape in the northern Sierra Nevada, Lake Tahoe Basin, California, USA. *For. Ecol. Manage.* **2008**, *255*, 707-719, doi:10.1016/j.foreco.2007.09.044.
- Martin-Benito, D.; Beeckman, H.; Cañellas, I. Influence of drought on tree rings and tracheid features of *Pinus nigra* and *Pinus sylvestris* in a mesic Mediterranean forest. *Eur. J. Forest Res.* **2013**, *132*, 33-45, doi:10.1007/s10342-012-0652-3.
- Meinzer, F.C.; McCulloh, K.A. Xylem recovery from drought-induced embolism: where is the hydraulic point of no return? *Tree Physiol.* **2013**, *33*, 331-334, doi:10.1093/treephys/tp022.
- Mayr, S.; Gruber, A.; Bauer, H. Repeated freeze-thaw cycles induce embolism in drought stressed conifers (Norway spruce, stone pine). *Planta* **2003**, *217*, 436-441, doi:10.1007/s00425-003-0997-4.
- Willson, C.J.; Jackson, R.B. Xylem cavitation caused by drought and freezing stress in four co-occurring *Juniperus* species. *Physiol. Plantarum* **2006**, *127*, 374-382, doi:10.1111/j.1399-3054.2006.00644.x.
- Fernández, M.E.; Gyenge, J.E.; de Urquiza, M.M.; Varela, S. Adaptability to climate change in forestry species: drought effects on growth and wood anatomy of ponderosa pines growing at different competition levels. *Forest Syst.* **2012**, *21*, 162-174, doi:10.5424/fs/2112211-12586.
- Ziaco, E.; Biondi, F.; Rossi, S.; Deslauriers, A. Intra-annual wood anatomical features of high-elevation conifers in the Great Basin, USA. *Dendrochronologia* **2014**, *32*, 303-312, doi:10.1016/j.dendro.2014.07.006.
- Domec, J.-C.; Pruyn, M.L.; Gartner, B.L. Axial and radial profiles in conductivities, water storage and native embolism in trunks of young and old-growth ponderosa pine trees. *Plant Cell Environ.* **2005**, *28*, 1103-1113, doi:10.1111/j.1365-3040.2005.01347.x.
- Martínez-Vilalta, J.; Sala, A.; Piñol, J. The hydraulic architecture of Pinaceae – a review. *Plant Ecol.* **2004**, *171*, 3-13, doi:10.1023/B:VEGE.0000029378.87169.b1.
- McDowell, N.G.; Pockman, W.T.; Allen, C.D.; Breshears, D.D.; Cobb, N.S.; Kolb, T.E.; Plaut, J.A.; Sperry, J.S.; West, A.; Williams, D.G.; et al. Mechanisms of plant survival and mortality during drought: why do some plants survive while others succumb to drought? *New Phytol.* **2008**, *178*, 719-739, doi:10.1111/j.1469-8137.2008.02436.x.
- Ziaco, E.; Biondi, F.; Rossi, S.; Deslauriers, A. Climatic influences on wood anatomy and tree-ring features of Great Basin conifers at a new mountain observatory. *Appl. Plant Sci.* **2014**, *2*, art. 1400054 (13 pp.), doi:10.3732/apps.1400054.

22. Ziaco, E.; Biondi, F.; Rossi, S.; Deslauriers, A. Environmental drivers of cambial phenology in Great Basin bristlecone pine. *Tree Physiol.* **2016**, *36*, 818-831, doi:10.1093/treephys/tpw006.
23. Ziaco, E.; Truettner, C.; Biondi, F.; Bullock, S. Moisture-driven xylogenesis in *Pinus ponderosa* from a Mojave Desert mountain reveals high phenological plasticity. *Plant Cell Environ.* **2018**, *41*, 823–836, doi:10.1111/pce.13152.
24. Maherali, H.; DeLucia, E.H. Xylem conductivity and vulnerability to cavitation of ponderosa pine growing in contrasting climates. *Tree Physiol.* **2000**, *20*, 859-867, doi:10.1093/treephys/20.13.859.
25. Domec, J.-C.; Gartner, B.L. Relationship between growth rates and xylem hydraulic characteristics in young, mature and old-growth ponderosa pine trees. *Plant Cell Environ.* **2003**, *26*, 471-483, doi:10.1046/j.1365-3040.2003.00978.x.
26. Pasques, O.; Munné-Bosch, S. Ancient trees are essential elements for high-mountain forest conservation: Linking the longevity of trees to their ecological function. *Proc. Nat. Acad. Sci.* **2024**, *121*, art. e2317866121 (11 pp.), doi:10.1073/pnas.2317866121.
27. Stephenson, N.L.; Das, A.J.; Condit, R.; Russo, S.E.; Baker, P.J.; Beckman, N.G.; Coomes, D.A.; Lines, E.R.; Morris, W.K.; Ruger, N.; et al. Rate of tree carbon accumulation increases continuously with tree size. *Nature* **2014**, *507*, 90–93, doi:10.1038/nature12914.
28. Hall, C.M.; James, M.; Baird, T. Forests and trees as charismatic mega-flora: implications for heritage tourism and conservation. *J. Heritage Tour.* **2011**, *6*, 309-323, doi:10.1080/1743873X.2011.620116.
29. Bernabei, M. The age of the olive trees in the Garden of Gethsemane. *J. Archaeol. Sci.* **2015**, *53*, 43-48, doi:10.1016/j.jas.2014.10.011.
30. Hansen, A.J.; Knight, R.L.; Marzluff, J.M.; Powell, S.; Brown, K.; Gude, P.H.; Jones, K. Effects of exurban development on biodiversity: Patterns, mechanisms, and research needs. *Ecol. Appl.* **2005**, *15*, 1893-1905, doi:10.1890/05-5221.
31. Grayson, D.K. *The Great Basin: A Natural Prehistory*, Revised and Expanded ed.; University of California Press: Berkeley, California, USA, 2011.
32. Stokes, M.A.; Smiley, T.L. *An Introduction to Tree-Ring Dating*, Reprint of the 1968 Edition ed.; University of Arizona Press: Tucson, Arizona, USA, 1996.
33. Holmes, R.L. Computer-assisted quality control in tree-ring dating and measurement. *Tree-Ring Bull.* **1983**, *43*, 69-78.
34. Frigo, D.; Römer, P.; Unterholzner, L.; Zimmer-Zachmann, H.; Esper, J.; Carrer, M.; Ziaco, E. Review of embedding and non-embedding techniques for quantitative wood anatomy. *Dendrochronologia* **2024**, *88*, 126241, doi:10.1016/j.dendro.2024.126241.
35. Guay, R.; Déry, A. *WinCELL 2020a for Wood Cell Analysis*; Regent Instruments Inc.: Quebec, Canada, 2020; p. 110.
36. Ziaco, E.; Liu, X.; Biondi, F. Dendroanatomy of xylem hydraulics in two pine species: Efficiency prevails on safety for basal area growth in drought-prone conditions. *Dendrochronologia* **2023**, *81*, art. 126116 (13 pp.), doi:10.1016/j.dendro.2023.126116.
37. Denne, M.P. Definition of latewood according to Mork (1928). *IAWA Bull. n.s.* **1988**, *10*, 59-62, doi:10.1163/22941932-90001112.
38. Menne, M.J.; Williams, C.N.; Gleason, B.E.; Rennie, J.J.; Lawrimore, J.H. The Global Historical Climatology Network Monthly Temperature Dataset, Version 4. *J. Clim.* **2018**, *31*, 9835-9854, doi:10.1175/jcli-d-18-0094.1.
39. Meko, D.M.; Biondi, F.; Taylor, A.H.; Panyushkina, I.P.; Thaxton, R.D.; Prusevich, A.A.; Shiklomanov, A.I.; Lammers, R.B.; Glidden, S. Runoff variability in the Truckee–Carson river basin from tree rings and a water balance model. *Earth Interact.* **2024**, *28*, art. e230018 (19 pp.), doi:10.1175/EI-D-23-0018.1.
40. Lopez-Saez, J.; Corona, C.; von Arx, G.; Fonti, P.; Slamova, L.; Stoffel, M. Tree-ring anatomy of *Pinus cembra* trees opens new avenues for climate reconstructions in the European Alps. *Sci. Total Environ.* **2023**, *855*, 158605, doi:10.1016/j.scitotenv.2022.158605.
41. Hipel, K.W.; McLeod, A.I. *Time Series Modelling of Water Resources and Environmental Systems*; Elsevier Science: Amsterdam, The Netherlands, 1994.
42. McLeod, A.I. *Package 'Kendall'*, 2.2.1; R Foundation for Statistical Computing: CRAN, 2025.

43. Zang, C.; Biondi, F. treeclim: an R package for the numerical calibration of proxy-climate relationships. *Ecography* **2015**, *38*, 431-436, doi:10.1111/ecog.01335.
44. Zang, C.; Biondi, F. Package 'treeclim', 2.0.7.1; R Foundation for Statistical Computing: 2025.
45. R Core Team R: *A language and environment for statistical computing*, 4.1.2; R Foundation for Statistical Computing: Vienna, Austria, 2021.
46. The MathWorks Inc. MATLAB. Available online: <https://www.mathworks.com> (accessed
47. Delwiche, L.D.; Slaughter, S.J. *The Little SAS Book: A Primer*, Sixth ed.; SAS Institute Inc.: Cary, North Carolina (USA), 2019.
48. Pacheco, A.; Camarero, J.J.; Carrer, M. Linking wood anatomy and xylogenesis allows pinpointing of climate and drought influences on growth of coexisting conifers in continental Mediterranean climate. *Tree Physiol.* **2016**, *36*, 502-512, doi:10.1093/treephys/tpv125.
49. Biondi, F.; Meko, D.M. Long-term hydroclimatic patterns in the Truckee-Carson Basin of the eastern Sierra Nevada, USA. *Water Resour. Res.* **2019**, *55*, 5559-5574, doi:10.1029/2019wr024735.
50. Gruber, A.; Strobl, S.; Veit, B.; Oberhuber, W. Impact of drought on the temporal dynamics of wood formation in *Pinus sylvestris*. *Tree Physiol.* **2010**, *30*, 490-501, doi:10.1093/treephys/tpq003.
51. Garcia-Forner, N.; Vieira, J.; Nabais, C.; Carvalho, A.; Martínez-Vilalta, J.; Campelo, F. Climatic and physiological regulation of the bimodal xylem formation pattern in *Pinus pinaster* saplings. *Tree Physiol.* **2019**, *39*, 2008-2018, doi:10.1093/treephys/tpz099.
52. Cuny, H.E.; Rathgeber, C.B.K. Xylogenesis: Coniferous trees of temperate forests are listening to the climate tale during the growing season but only remember the last words! *Plant Physiol.* **2016**, *171*, 306-317, doi:10.1104/pp.16.00037.
53. Stewart, I.T.; Cayan, D.R.; Dettinger, M.D. Changes toward earlier streamflow timing across western North America. *J. Clim.* **2005**, *18*, 1136-1155, doi:10.1175/JCLI3321.1.
54. Knowles, N.; Dettinger, M.D.; Cayan, D.R. Trends in snowfall versus rainfall in the western United States. *J. Clim.* **2006**, *19*, 4545-4559, doi:10.1175/JCLI3850.1.
55. Painter, T.H.; Skiles, S.M.; Deems, J.S.; Brandt, W.T.; Dozier, J. Variation in rising limb of Colorado River snowmelt runoff hydrograph controlled by dust radiative forcing in snow. *Geophys. Res. Lett.* **2018**, *45*, 797-808, doi:10.1002/2017GL075826.

Disclaimer/Publisher's Note: The statements, opinions and data contained in all publications are solely those of the individual author(s) and contributor(s) and not of MDPI and/or the editor(s). MDPI and/or the editor(s) disclaim responsibility for any injury to people or property resulting from any ideas, methods, instructions or products referred to in the content.